IVYSPRING
INTERNATIONAL PUBLISHER

Theranostics

Research Paper

Glioma Dual-Targeting Nanohybrid Protein Toxin Constructed by Intein-Mediated Site-Specific Ligation for Multistage Booster Delivery

Yingzhi Chen[1, 2], Meng Zhang[1, 2], Hongyue Jin[1, 2], Dongdong Li[1,3], Fan Xu[1,3], Aihua Wu[1], Jinyu Wang[1], and Yongzhuo Huang[1✉]

1. Shanghai Institute of Materia Medica, Chinese Academy of Sciences. 501 Haike Rd, Shanghai 201203, China
2. University of Chinese Academy of Sciences. 19A Yuquan Road, Beijing 100049, China
3. Nano Science and Technology Institute, University of Science and Technology of China. 166 Ren-ai Rd, Suzhou 215123, China

✉ Corresponding author: HUANG, Yongzhuo, Ph.D., Professor of Pharmaceutics, Shanghai Institute of Materia Medica, Chinese Academy of Sciences, 501 Hai-ke Rd, Shanghai 201203; Tel +86-21-20231000 ext 1401; Fax: +86-21-20231981; Email: yzhuang@simm.ac.cn

Abstract

Malignant glioma is one of the most untreatable cancers because of the formidable blood–brain barrier (BBB), through which few therapeutics can penetrate and reach the tumors. Biologics have been booming in cancer therapy in the past two decades, but their application in brain tumor has long been ignored due to the impermeable nature of BBB against effective delivery of biologics. Indeed, it is a long unsolved problem for brain delivery of macromolecular drugs, which becomes the Holy Grail in medical and pharmaceutical sciences. Even assisting by targeting ligands, protein brain delivery still remains challenging because of the synthesis difficulties of ligand-modified proteins. Herein, we propose a rocket-like, multistage booster delivery system of a protein toxin, trichosanthin (TCS), for antiglioma treatment. TCS is a ribosome-inactivating protein with the potent activity against various solid tumors but lack of specific action and cell penetration ability. To overcome the challenge of its poor druggability and site-specific modification, intein-mediated ligation was applied, by which a gelatinase-cleavable peptide and cell-penetrating peptide (CPP)-fused recombinant TCS toxin can be site-specifically conjugated to lactoferrin (LF), thus constructing a BBB-penetrating, gelatinase-activatable cell-penetrating nanohybrid TCS toxin. This nanohybrid TCS system is featured by the multistage booster strategy for glioma dual-targeting delivery. First, LF can target to the BBB-overexpressing low-density lipoprotein receptor-related protein-1 (LRP-1), and assist with BBB penetration. Second, once reaching the tumor site, the gelatinase-cleavable peptide acts as a separator responsive to the glioma-associated matrix metalloproteinases (MMPs), thus releasing to the CPP-fused toxin. Third, CPP mediates intratumoral and intracellular penetration of TCS toxin, thereby enhancing its antitumor activity. The BBB penetration and MMP-2-activability of this delivery system were demonstrated. The antiglioma activity was evaluated in the subcutaneous and orthotopic animal models. Our work provides a useful protocol for improving the druggability of such class of protein toxins and promoting their *in-vivo* application for targeted cancer therapy.

Key words: trichosanthin, lactoferrin, brain targeted delivery, antiglioma therapy, MMP-2, intein-mediated protein ligation, cell-penetrating peptide

Introduction

The formidable blood–brain barrier (BBB) imposes the primary challenge for pharmacotherapy of brain tumors, in which there are very few BBB-permeable drugs available for clinic. Given the ominous biological obstacle, macromolecular therapy via systemic delivery is virtually inapplicable for brain cancer. Generally, there are multiple bio-barriers against a drug reaching the cancer cells. First, serving as a major component of the BBB, the cerebral microvessel endothelial cells are characterized by the high expression of the tight junction proteins and the poor transcellular

endocytosis.[1] For example, the transendothelial electrical resistance of brain microvessels is 100–500 fold higher than the non-cerebral capillaries.[2] Second, poor intratissue penetration severely restricts drugs reaching the targeting cells. The diffusion coefficient of macromolecules with a size of approximate 20 kDa in the brain is estimated to be around 10^{-6} cm^2/s, and it would take roughly 3 days for 1-mm distance diffusion.[2] Third, a major class of therapeutics must enter the cells for taking action, and the cell membrane imposes a barrier for those such as protein toxins due to the lack of cell-penetrating ability.

Therefore, it is required to overcome all these bio-barriers simultaneously so as to achieve effective brain delivery, and if delivery fails in any step in the process, the therapy will be ineffectual. We proposed the formula to describe the efficiency of brain tumor delivery.

$$Delivery\ efficiency = E_{BBB} \times E_{diffusion} \times E_{cell}$$

where E_{BBB}, $E_{diffusion}$, and E_{cell} represent the efficiency of BBB penetration, intratumoral infiltration, and intracellular delivery, respectively.

Such a multi-step process imposes the rigid requirements and big challenges for brain delivery design, and thereby every delivery step should be taken into account to achieve an optimal efficiency. To complete this complicated delivery task, a multipronged system must bear various specific functions targeting each barrier.

Currently, brain delivery investigations have mainly focused on how to overcome the BBB. However, as discussed above, for macromolecular drugs, the BBB penetration is not a guaranty of effective therapy, because of the intra-brain delivery barriers. Herein, we proposed a multistage booster delivery strategy, by which a brain-targeting, protease-activatable cell-penetrating delivery system of protein toxin trichosanthin (TCS) was developed for antiglioma therapy.

TCS is a ribosome-inactivating protein (RIP), derived from the Chinese herb *Tian Hua Fen*, the root of *Trichosanthes kirilowii Maxim*. TCS is a gynaecological drug approved in China for use in ectopic pregnancies, hydatidiform moles, chorionic epithelioma, and abortion.[3] For our interest, TCS has been reported to have high antitumor activity via ribosome-inactivating mechanism, thus with great promise for cancer therapy.[4] Theoretically, a single RIP molecule can kill one cell once it enters the cytosol, whereas it usually takes 10^4–10^5 small molecular drugs to achieve the same task.[5] Moreover, TCS can induce cell apoptosis through various mechanisms.[6-8] However, TCS has short

half-life owing to rapid renal clearance related to its relative small size (27 kDa), and is poorly cell permeable.[3, 9] Furthermore, due to its BBB-impermeability, TCS has not been investigated on brain cancer therapy. It thus serves as an ideal macromolecular model in demonstrating our proposed delivery strategy.

We developed a rocket-like, multistage booster delivery system for TCS (Scheme 1). This hybrid system incorporated three functional motifs onto TCS: a cell-penetrating peptide (CPP) (i.e., low-molecular weight protamine, LMWP), a matrix metalloproteinases (MMP) substrate peptide (MSP), and a brain-targeting ligand lactoferrin (LF). Such a protein nanohybrid displayed multistage delivery features. Specifically, LF functions as a first-stage booster, which can selectively bind to low-density lipoprotein-related protein-1 (LRP-1) overexpressed on brain capillary endothelial cells,[10] and thus mediate BBB penetration. Subsequently, once reaching the tumor site, the protease cleavable linker MSP serves as a separator, which can be recognized and cleaved by the tumor-associated MMPs, and thus rTCS-LMWP is released. Finally, the exposed cell-penetrating LMWP works as the second-stage booster for promoting TCS (warhead) intratumoral infiltration and penetration into glioma cells, exerting its antitumor activity.

However, it is difficult to synthesize such a complicated system. Specifically, TCS is small size protein (27 kDa) and random modification could reduce its activities. To achieve site-specific modification, we developed a highly efficient yet easily processed method based on intein-mediated protein ligation (IPL) for the protein toxin drug.

Results

IPL has been developed for untagged protein expression and protein modification,[11, 12] but IPL has been rarely reported for use in protein toxin drug development. The toxin-intein fusion protein is subjected to thiol-induced cleavage, yielding an active thioester or thiol at the C-terminus. The thioester or thiol group can be further used for site-specific conjugation with any modifier bearing sulfide group or maleimide (**Figure 1A**). An advantage of this technique is that the protein purification, activation and conjugation can be done with one or two-step on-column process. Of note, the cysteine in the intein-fused protein is protected in a form of thioester, and becomes available as the terminal cysteine only after intein-mediated on-column cleavage. As a comparison, the conventional method of direct introducing cysteine at the protein terminus is vulnerable to oxidation and prone to form the

intermolecular dimers during protein production processes.

The genetically engineered proteins of intein-CBD-fused rTCS and rTCS-LMWP-MSP (rTLM) were expressed in *E.coli*, and purified via the intein-CBD tag binding with chitin-binding affinity column. The intein-mediated, cysteine-inducing cleavage was performed on-column to yield a C-terminal cysteine on the protein (i.e., rTCS or rTLM) (**Figure 1A**). The rTLM-LF was prepared using a hetero-bifunctional cross-linker NHS-PEG$_{3500}$-MAL (**Figure 1B**).

The purified rTCS and rTLM showed the molecular mass of 27 and 30 kDa, respectively (**Figure 1C**), consistent with their theoretical molecular weight. The calculated isoelectric point (pI) of rTLM and LF were 10 and 8, respectively, indicating the pI of the rTLM-LF should be 8–10. The cation-exchange chromatography was thus used to separate rTLM-LF from the unreacted rTLM and LF. Under pH 8.0, the electrically neutral LF protein flowed through the column, while the rTLM-LF and rTLM were successively eluted from the column by running a salt gradient buffer (**Figure 1D**). The purified rTLM-LF was characterized by SDS-PAGE electrophoresis, showing a band of approximately 120 kDa (**Figure 1E**). Of note, the rTLM-LF contained a PEG crosslinker, and PEG usually causes a broad band on the SDS-PAGE.
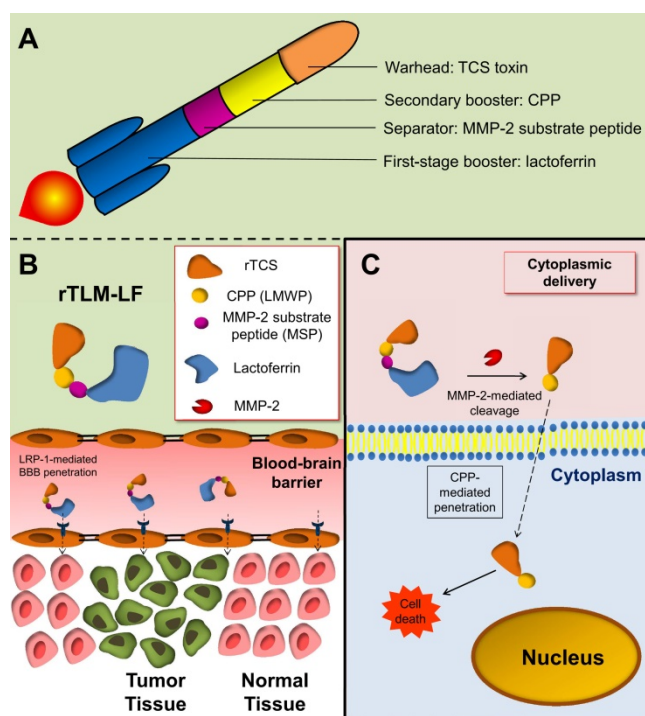
Scheme 1. Illustration of the rocket-like, multi-stage booster delivery strategy of the BBB-penetrating nanohybrid TCS toxin for antiglioma treatment.

The rTLM-LF was visualized using atomic force microscopy (AFM). The nanohybrid structure was clearly seen in the AFM images (**Figure 1F**), showing two protein combination. It should be noted that the AFM imaging could be affected by the position manner of the two components of the hybrid. For example, if they positioned side-by-side, there would show clear combination structure. But when they positioned at an up-and-down overlap manner, there could show a single one. The nanohybrid protein rTLM-LF was stable at room temperature for over 72 h.

LF-mediated penetration across the BBB represents the first-stage booster function of the brain-targeting protein toxin delivery system, which was evaluated using an *in-vitro* BBB Transwell-based model with BCEC cells (LRP-1 overexpression) in the upper chamber and GL261 murine glioma cells in the lower chamber (**Figure 2A** and **2B**). The rTLM-LF showed the remarkably enhanced cellular uptake in GL261 cells compared to rTCS in both the flow cytometry (**Figure 2C**) and fluorescent imaging results (**Figure 2F**). Furthermore, the uptake enhancement in BCEC cells was also found in the rTLM-LF group (**Figure 2D** and **Figure 2G**). In addition, the enhanced uptake in both the Transwell-based model and BCEC cells could be inhibited by pretreatment with either the natural substrate of LRP-1 (*i.e.*, low-density lipoprotein, LDL) or free LF protein (**Figure 2C–G**). The quantitative analysis of the flow cytometry results was shown in **Figure 2E**. These pilot results demonstrated the ability of LF-mediated BBB penetration of protein drugs.

After permeating the BBB and reaching tumor site, the rTLM-LF would expose to the tumor-associated MMP-2, and the substrate-linker MSP then be cleaved. MSP thus serves as a separator. The first-staging booster LF is discarded, and the cell-penetrating TCS-LMWP released. LMWP is a naturally-sourced cell-penetrating sequence, derived from a clinical drug protamine by enzyme digestion.[13] LMWP has been applied in our lab as potent CPP for promoting cancer drug delivery for overcoming barriers against intratumoral and intracellular delivery.[14, 15]

To demonstrate the separator (MSP) and second-stage booster (LMWP) function of the rocket-like system, the FITC-labeled rTLM-LF was pretreated by GL261 cell-conditioned medium containing the secreted MMPs and then given to the cells. The pretreated rTLM-LF showed the enhanced cellular uptake compared to the non-pretreated control group in both the glioma cell lines (C6 and GL261), evaluated by fluorescent imaging (**Figure 3A, B**) and flow cytometry (**Figure 3C**, **D**). The similar

results were also observed in other solid tumor cell lines (e.g., HeLa and MCF-7) (**Figure 3E, H**). These results demonstrated the success of MMP-triggered detachment of the first-stage booster LF protein, thus launching the CPP-mediated second-stage booster for intracellular delivery of TCS toxin.

The unmodified rTCS showed the similar cytotoxicity in the two murine glioma cell lines C6 and GL261, with the IC_{50} value of 10.4 and 14.2 μM, respectively. The rTLM without LF modification showed the enhanced cytotoxicity in both cell lines, with the IC_{50} values of 4.7 and 0.50 μM, respectively, presumably due to the non-selective CPP-mediated cellular uptake. By sharp contrast, the rTLM-LF showed the IC_{50} values of 17.3 and 0.37 μM in C6 and GL261 cells, respectively, and there was a 46-fold

difference in cytotoxicity between them (**Figure 4A, B**). It was due to the high level of MMP-2 in GL261, but not in C6 cells (**Figure 4D**). The rTLM-LF was efficiently cleaved by the GL261-conditioned medium containing high level of MMP-2, leading to the release of rTCS-LMWP (**Figure 4E**). The cleavage efficiency was approximately 92%, calculated by gray scale analysis using ImageJ. The rTLM-LF also showed less toxicity to the normal cells, such as BCEC (**Figure S1B**) and HUVEC (**Figure S1B**), which had low MMP-2 expression level (**Figure S1C**). The results demonstrated that the rTLM-LF was effectively activated by the tumor-associated MMP-2, and thus could take targeting action on the MMP-expressed cancer cells and spare the normal cells.
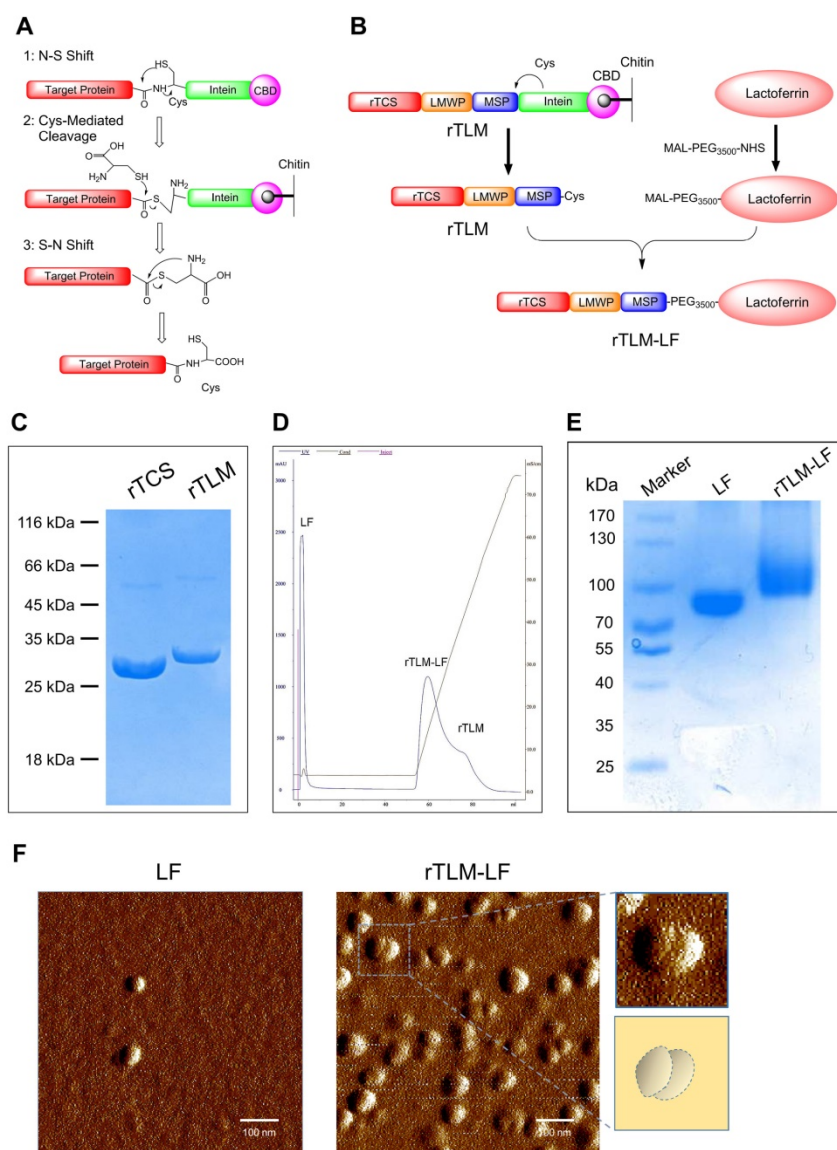

Figure 1. Preparation of rTLM-LF hybrid toxin. (A) Scheme of intein-mediated protein ligation. (B) Synthesis of rTLM-LF hybrid toxin. (C) SDS-PAGE characterization of the rTLM protein. (D) Separation of rTLM-LF using cation-exchange chromatography. (E) SDS-PAGE characterization of rTLM-LF. (F) AFM images of the protein hybrid.

Of interest, rTLM-LF showed less cytotoxicity in the MMP-negative C6 cells than the unmodified rTCS (IC$_{50}$: 17.3 µM *vs* 10.4 µM). However, there was an opposite situation in the MMP-expressed GL261 cells, the cytotoxicity of rTLM-LF was significantly enhanced, compared to the unmodified rTCS (IC$_{50}$: 0.37 µM *vs* 14.2 µM). The rTLM-LF could be delivered into both cell lines through LRP-1 receptor, because the reduced uptake was observed after pretreatment with free LF (**Figure S2A, B**), and both cell lines expressed LRP-1 (**Figure S2C**). Although the cellular uptake of rTLM-LF in C6 and GL261 was similar, it was significantly lower than that of unmodified rTLM (**Figure S2A, B**), demonstrating CPP-mediated cell penetration was more efficient than LRP-1 receptor-mediated uptake in the glioma cells. Due to the incapability of extracellular cleavage and release

of rTCS-LMWP, the rTLM-LF had low cytotoxicity in C6 cells. It clearly revealed the benefit of LMWP-promoting cellular uptake under the circumstance of MMP-triggered cleavage of rTLM-LF and release of rTCS-LMWP. In addition, the LF protein exhibited little cytotoxicity in both cell lines at a concentration up to 10 µM (**Figure 4C**).

Of note, although the C6 and BCEC cells had high levels of LRP-1 that might potentially increase the uptake, rTLM-LF could not be cleaved and release rTCS-LMWP to exert cytotoxicity because both cell lines had low MMP-2 level (**Figure S1C**). For GL261 cells, the enhanced toxicity was presumably due to the effective extracellular cleavage and activation by the secreted MMP-2 and the consequent increased cellular uptake.
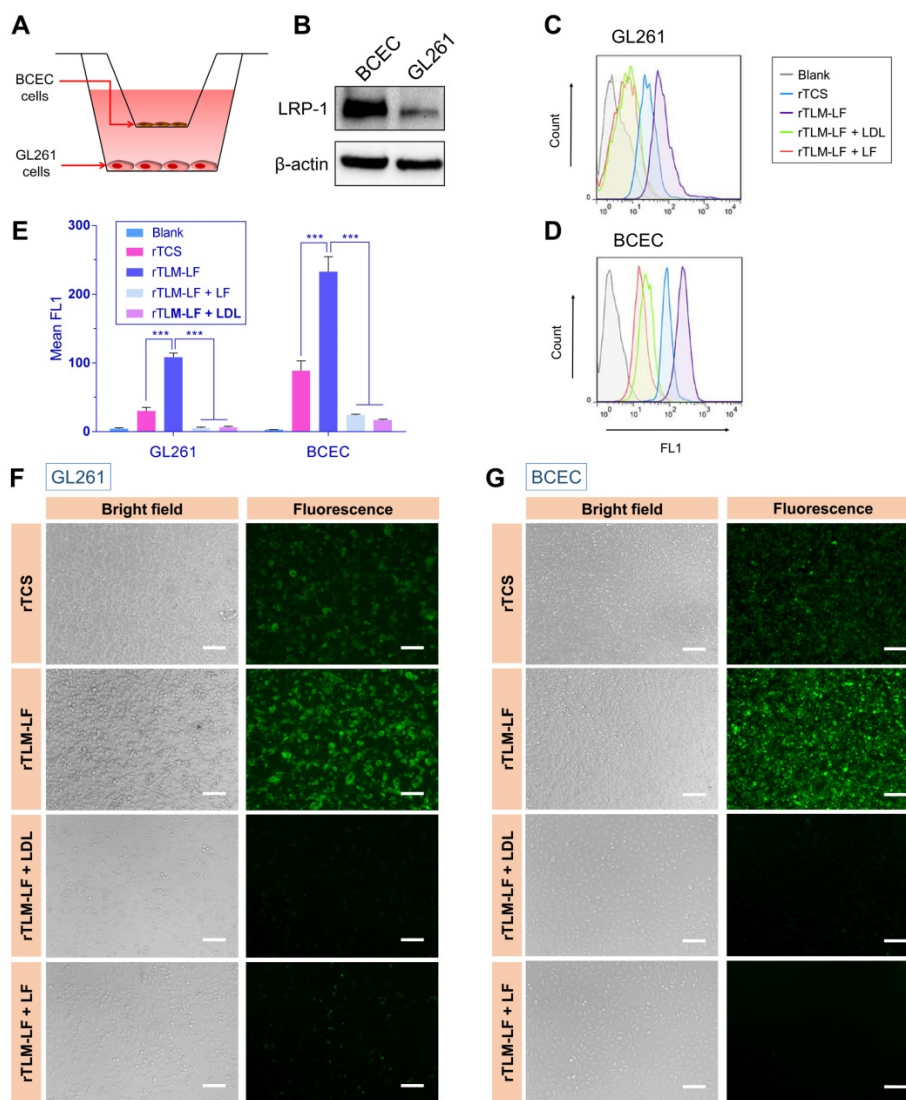

Figure 2. Evaluation of rTLM-LF penetration across BBB. (A) Scheme of the Transwell model. (B) LRP-1 expression in BCEC and GL261 cells. (C) Flow cytometry and (F) fluorescent imaging of rTCS and rTLM-LF uptake in GL261 cells in the Transwell model with and without pretreatment of LDL and LF. (D) Flow cytometry and (G) fluorescent imaging of rTCS and rTLM-LF cellular uptake in BCEC cells with and without pretreated by LDL and LF. (E) Quantitative analysis of the flow cytometry results. (Scale bar, 50 µm) Statistical analysis was conducted using one-way ANOVA test by GraphPad Prism. ***p<0.001.
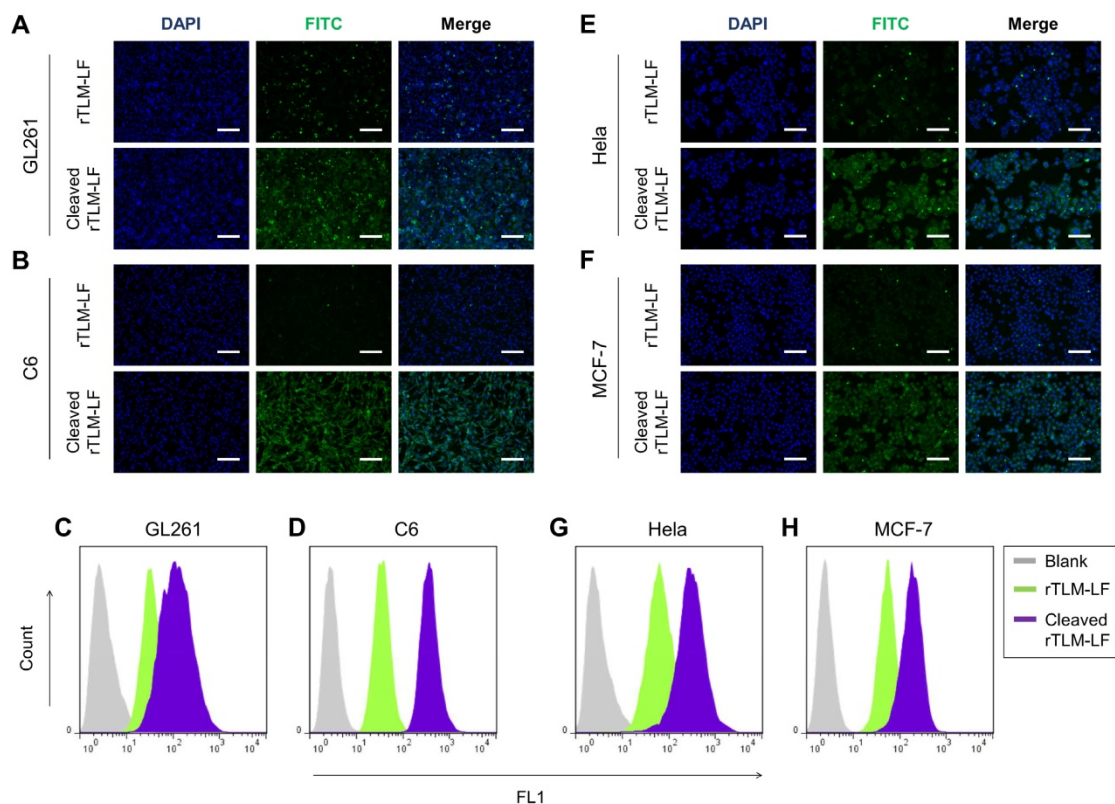
Figure 3. MMP-2-mediated cellular uptake. (A, B) Fluorescent imaging and (C, D) flow cytometry analysis of the uncleaved/pre-cleaved rTLM-LF uptake in C6 and GL261 cells. (E, F) Fluorescent imaging and (G, H) flow cytometry analysis of the uncleaved/pre-cleaved rTLM-LF uptake in HeLa and MCF-7 cells. (Scale bar, 50 μm)
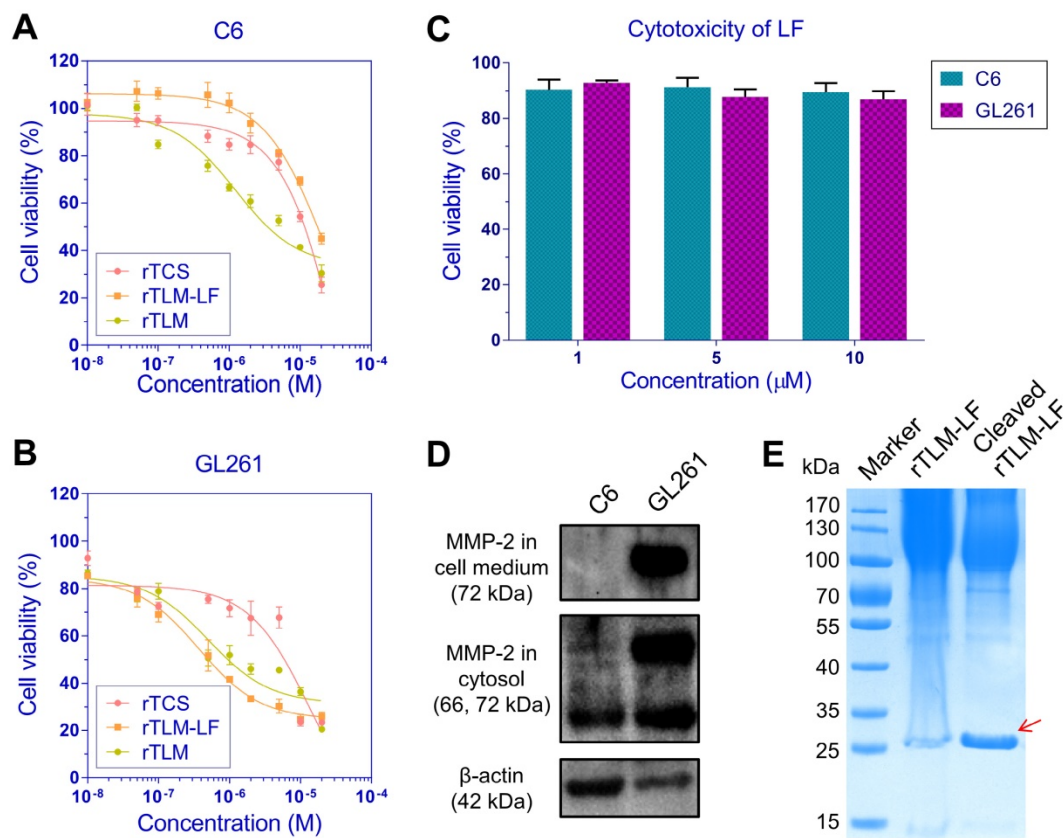

Figure 4. MMP-2-mediated cytotoxicity. Cytotoxicity of rTCS and rTLM-LF in (A) C6 and (B) GL261 cells. (C) Cytotoxicity of LF protein in C6 and GL261 cells. (D) Cellular MMP-2 expression and secretion level detected in C6 and GL261 cells. (E) MMP-2-mediated cleavage of rTLM-LF using GL261-conditioned medium.

The *in-vivo* targeting of rTLM-LF was evaluated using an orthotopic GL261 glioma animal model by tail injection of the Cy5-labeled rTLM-LF and rTCS. The fluorescent imaging showed that rTLM-LF efficiently accumulated at the brain, with better brain-targeting effect than the unmodified rTCS (**Figure 5A**). The tissue distribution results revealed that both rTLM-LF and rTCS had a high accumulation level in the liver and kidney, which are known as the major organs for protein drug metabolism and excretion, respectively (**Figure 5B**). The glioma accumulation of the non-modified rTCS also suggested that the ERP effect was an important mechanism for brain tumor targeting.

The cryosection slices of the orthotopic GL261 glioma tumor tissues were observed for further confirmation of the glioma targeting of rTLM-LF. The results demonstrated the deep penetration into the tumor, presumably due to the LMWP-facilitated infiltration (**Figure 5C**). In our previous work, LMWP-mediated delivery was also found with enhanced intratumoral penetration.[14-15] However, little is known about its mechanisms of intra-tissue penetration, and we speculated that CPP could enhance the tumor uptake, as well as penetration via a possible mechanism of saturation of layer by layer. In addition, the reduced size was also beneficial for the intraglioma diffusion of the LF-removed rTLM. The immunofluorescent staining of LRP-1 receptor showed colocalization of the Cy5-labeled rTLM-LF and LRP-1 in the brain tissue (**Figure 5E**), demonstrating the ability of LF-mediated brain targeting. The CPP-mediated delivery could increase the drug accumulation in the tumor cells than the normal brain cells, and thus render the brighter spots in the glioma and deep penetration.
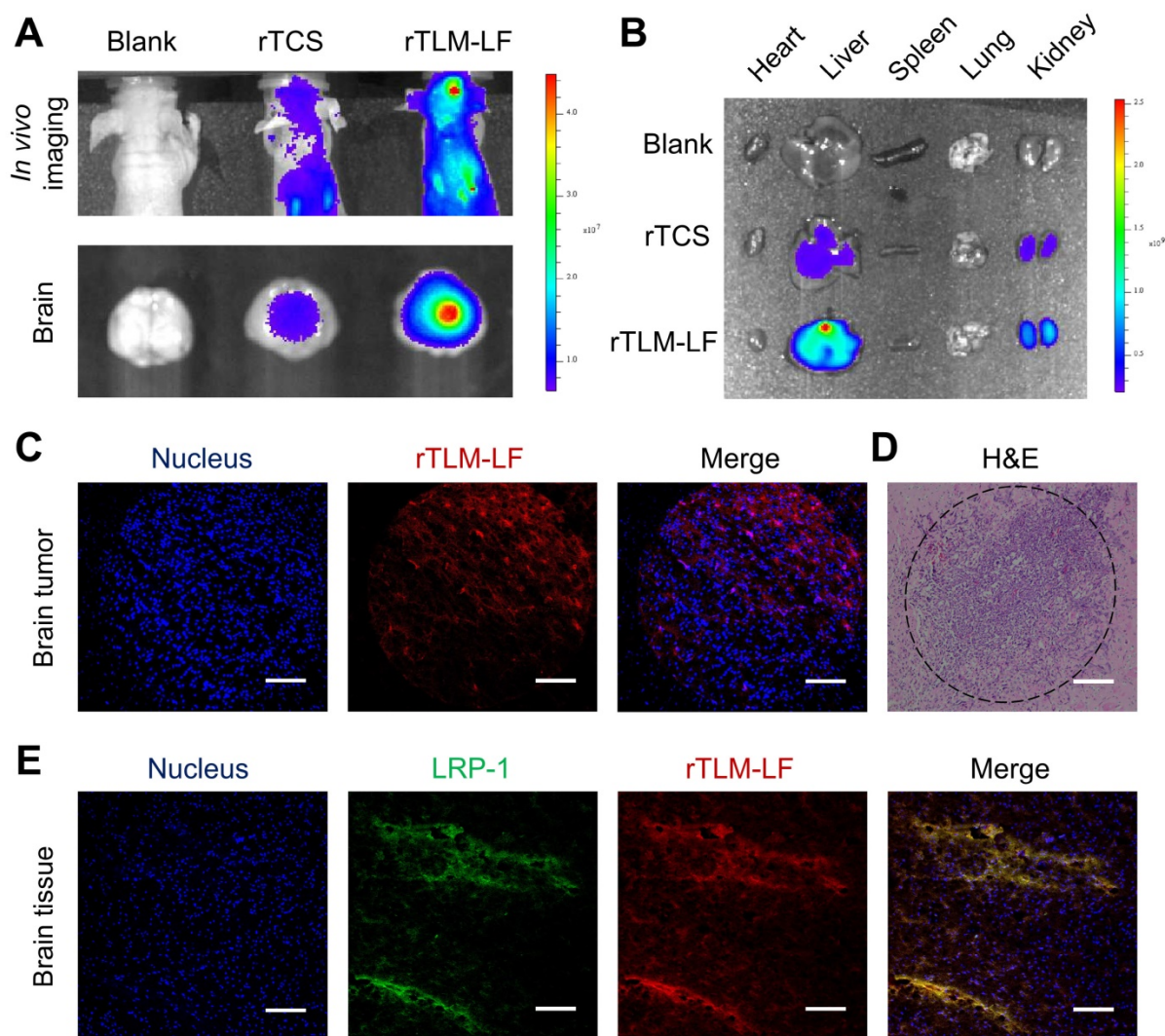

Figure 5. *In vivo* glioma targeting evaluation. (A) Fluorescent imaging of brain targeting of Cy5-labeled rTCS and rTLM-LF 24 h after tail injection. (B) Fluorescent imaging of tissue distribution. (C) Confocal imaging of the brain tumor cryosection. (D) H&E staining of the brain tumor paraffin section. (E) Confocal imaging of LRP-1 immunofluorescent staining of the brain tissue cryosection. (Scale bar, 100 μm)

The antiglioma treatment was first performed using the nude mouse model harboring subcutaneous GL261 tumor xenografts. The rTLM-LF showed greater efficacy on tumor growth suppression than rTCS (**Figure 6A-C**). However, it should be noted that the treatment efficacy by rTLM-LF just displayed moderate improvement compared to rTCS. These results could be explained that LF-mediated targeting did not play an important role in the subcutaneous tumor model. Although the MMP-2 level in GL261 was as high as in the HT1080 tumor (**Figure 6E**), GL261 subcutaneous tumor had very low LRP-1 expression (**Figure 6F**). By contrast, LRP-1 receptor was highly expressed in the BBB-associated BCEC and bEnd.3 cells, but very low in the normal endothelial HUVEC cells (**Figure S3**, Supporting Information). Hence, the LF-mediated first-staging booster of the rTLM-LF delivery system could not be effectively functioned in the subcutaneous tumor model, and an increased dose might not lead to significant drug tumor accumulation.

Interestingly, the significantly improved therapeutic efficacy was found in the subcutaneous GL261-bearing immunocompetent C57BL/6 mouse model (**Figure 7A-C**), compared to the nude mouse model. The tumor growth inhibition rate was 51 and 78% for rTCS and rTLM-LF, respectively. Since TCS toxin was reported to enhance antitumor immune response by recruiting CD8+ T cells in the lung tumor-bearing mice,[16] we examined the percentage of T cells, particularly CD8+ T cells, in the lymph node and spleen of the treated animals. There was no major difference of CD8+ T cell percentage in the lymph nodes among different groups, but a significant increase in the spleens from the rTCS- and rTLM-LF-treated group compared to the saline control (**Figure 7D, E**). Furthermore, the immunohistochemistry staining of CD8α showed enhanced CD8+ T cell infiltration into the tumor tissue after rTCS and rTLM-LF treatment (**Figure 7F**), suggesting the CD8+ T cell infiltration was involved in the antitumor effects.

We further tested the treatment using an orthotopic GL261-bearing immunocompetent C57BL/6 mouse model. The rTCS-treated group showed the median survival time of 12.5 days (p<0.05 *vs* saline control group), and the last survival was 19 days. The rTLM-LF treatment showed the median survival time of 19 days (p<0.001 *vs* saline control group; p<0.01 *vs* rTCS group) (**Figure 8A**). In another parallel experiment, the orthotopic GL261-xenografted mice were treated for consecutive three days, and the brain tissues were dissected for the H&E staining to compare the orthotopic glioma size. The results showed significant shrinkage of the orthotopic glioma in the rTCS and rTLM-LF groups compared to the saline control group, while the smallest glioma size was found in the rTLM-LF group (**Figure 8C**), indicating rTLM-LF greatly improved the efficacy of glioma treatment.
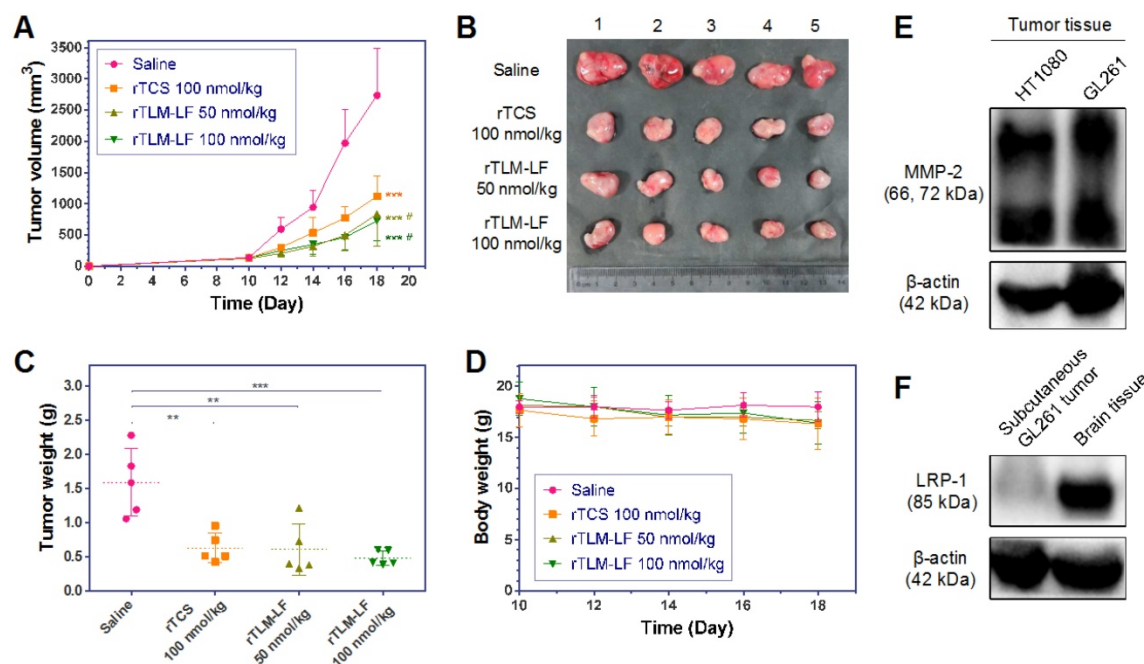

Figure 6. Antiglioma treatment in the subcutaneous GL261-xenografted nude mice model. (A) Tumor growth curve, (B) tumor images, and (C) tumor weight of the animals treated with saline, rTCS and rTLM-LF. (D) Animal body weight change during the treatment. (E) MMP-2 level in the HT1080 and GL261 tumor tissue. (F) LRP-1 level in the subcutaneous GL261 tumor and mouse brain tissue. (* p<0.05; ** p<0.01; *** p<0.001 *vs* saline control group. # p<0.05 *vs* rTCS group. n = 5)
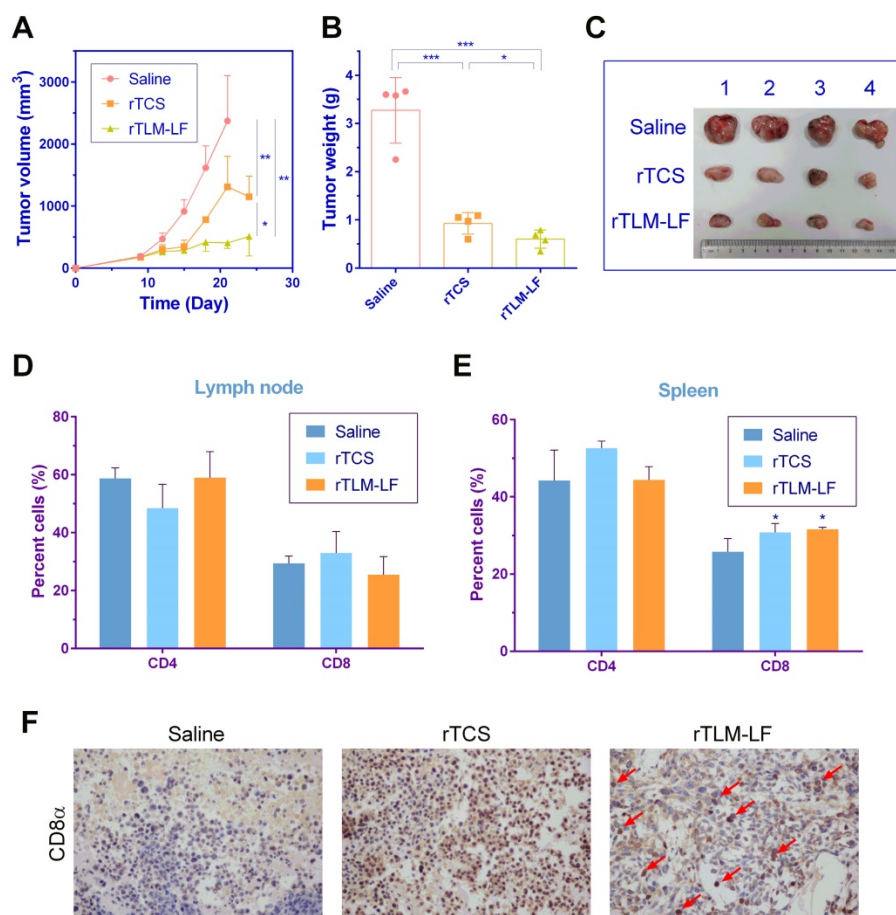
Figure 7. Antiglioma treatment in the subcutaneous GL261-xenografted C57 mouse model. (A) Tumor growth curve, (B) tumor weight and (C) tumor images of the animals treated with saline, rTCS and rTLM-LF. Percentage of CD4+ and CD8+ T cells in (D) lymph node and (E) spleen of the treated animals at the endpoint measured by flow cytometry. (F) Immunohistochemistry staining of CD8α in tumor tissues. (* $p<0.05$; ** $p<0.01$; *** $p<0.001$)

The H&E staining of the major organs was shown in **Figure 8D** that rTCS had severe pathologic toxicity in multiple organs. Specifically, the pathologic symptoms included: disarrangement of hepatic cells and hemorrhage in the liver; abnormal proliferation of capillary and hemorrhage in the spleen; increased thickness of the alveolar walls and disarrangement of epithelial cells in the lung; disarrangement and swelling of convoluted tubules and glomerular in the kidney. By contrast, the safety and biocompatibility were greatly improved in the rTLM-LF-treated mice.

Because the protein drugs typically had considerable accumulation in the liver, the plasma levels of aspartate aminotransferase (AST)/alanine aminotransferase (ALT) and alkaline phosphatase (ALP) were measured. AST/ALT and ALP are the important biochemical parameters for hepatotoxicity evaluation. There was no significant change in AST/ALT level among the groups (**Figure 8E**), but the ALP level in rTCS-treated mice was much higher than either the healthy mice or the saline control group. No significant increase was found in the rTLM-LF group

(**Figure 8F**), indicating rTLM-LF had less hepatotoxicity than rTCS. Taken together, these results indicated rTLM-LF had less systematic toxicity than rTCS due to its increased brain tumor targeting, as well as the MMP-activatable property.

TCS protein has severe immunogenicity, which raises potential safety concerns in clinical use.[17] To evaluate the immunogenicity of the rTLM-LF in comparison with rTCS and PEGylated rTCS, the Balb/c mice were subcutaneously immunized with these agents for three times with one-week interval. One week after the last immunization, the plasma anti-TCS IgG level was thus measured using ELISA assay. The rTLM-LF showed significant reduction of immunogenicity, similar to the rTCS-PEG control (**Figure 8G**). The titer of the neutralizing antibody was reduced to 5,000, compared to the higher level of 50,000 in the rTCS group. This was presumably because the large LF protein effectively shielded the immunogenic epitope of rTCS. This result provided another evidence of the enhanced biosafety of the multi-step booster delivery system rTLM-LF compared with unmodified rTCS toxin.
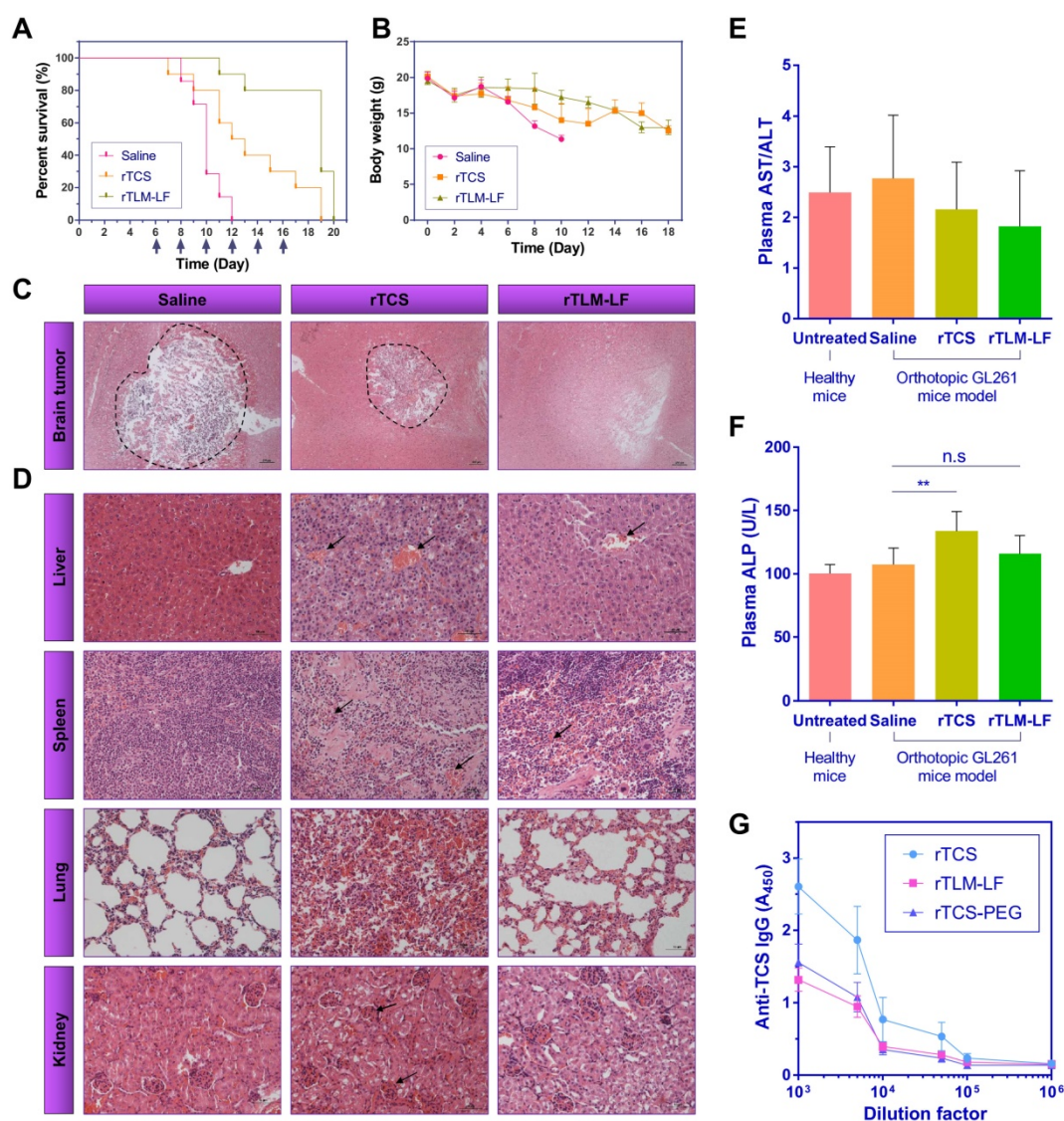
Figure 8. Antiglioma treatment in the orthotopic GL261-xenografted mouse model. (A) Survival curve and (B) animal body weight changes of the animals treated with saline (n=7), rTCS (n=10) and rTLM-LF (n=10). H&E staining of (C) the brain tumors and (D) major organs of the treated animals. (E) Plasma AST/ALT and (F) ALP levels of the treated animals. (G) Plasma anti-TCS IgG level in the Balb/c mice subcutaneously immunized by rTCS, rTLM-LF and rTCS-PEG. (* $p<0.05$; ** $p<0.01$; *** $p<0.001$; *n.s.* no significance)

Discussion

Because of the poor druggability, the clinical use of protein toxins has been severely constrained despite their potent anti-cancer activity.[18] Targeted delivery of protein toxins to tumor cells is still a real challenge, but on the other hand, the introduction of advanced delivery techniques represents an opportunity to re-examine the therapeutic application of these proteins, for instance, in antiglioma.

Macromolecular brain delivery is a long-sought goal in medical society and pharmaceutical industry. Effective brain delivery typically encounters various barriers sequentially. Therefore, to design a protein brain delivery system, every single barrier must be taken into account and specifically addressed. We

thus developed a rocket-like, multistage booster delivery strategy with protease-activatable property.

Targeting to the upregulated signals (e.g., ROS) and proteases in cancer cells offers a potential method to improve tumor-specific action of drugs.[19, 20] This system was characterized by dual-targeting functions via LF-mediated BBB penetration and MMPs-activatable cell penetration. It has been well demonstrated the effectiveness of LF protein in the nanoparticulate delivery systems for penetrating BBB via LRP-1 receptor-mediated endocytosis,[21, 22] yet it has been rarely reported in protein brain delivery. Meanwhile, as an endogenous protein, LF is easily available and does not raise safety concerns. Therefore, LF can ideally serve as the targeting molecule and the first-stage booster to target the BBB.

Once the BBB-penetrating nanohybrid protein toxin reaches the glioma, LF could be specifically cleaved from the system by the glioma-associated MMP-2 to release the CPP-fused TCS toxin. The MMP-2-activable prodrug-like property reduced the side toxicity to the normal cells because the large LF motif blocked the active site of TCS as long as they were in a nanohybrid form. As the formula to describe the brain delivery efficiency we propose above, three factors govern the delivery efficiency. Among them, intratumoral diffusion has been largely ignored to specifically address in the delivery system design. To some degree, this might not be a crucial rate-limited step for small drugs that readily diffuse in a concentration-driven pattern, but it turns essentially important for proteins due to their restraining from free diffusion in brain tissues.[2] Therefore, the primary targeting to the BBB via LF/LRP-1 interaction can address the factor of E_{BBB}, and the secondary targeting by MMPs-activation can address the factors of $E_{difffusion}$ and E_{cell} via CPP-mediated intratumoral and intracellular penetration.

A convenience of this nanohybrid protein system is that the MMP-substrate linker can be readily replaced with another protease-cleavable sequence by recombinant method, thus rendering the system adaptable to various tumor microenvironments, with potential to achieve precise therapy.

Of note, an intein-mediated protein ligation strategy was used to construct such a complex multi-stage booster delivery system. The intein-based method has been developed for years, and used for protein expression, labeling and conjugation due to the facile operation and high efficiency.[11] But its application in construction of protein drug delivery system has virtually unexplored. We have previously succeeded in developing a method for intein-mediated site-specific PEGylation of protein toxin.[23, 24] In this work, we applied this strategy to achieve the site-specific modification of rTLM with LF to construct a BBB-penetrating nanohybrid protein toxin for antiglioma treatment. This method could offer a facile protocol for enhanced delivery of protein toxins for improving cancer treatment outcomes.

Conclusions

In summary, we developed a site-specific modification platform for constructing a rocket-like, multi-stage booster strategy of the BBB-penetrating nanohybrid TCS toxin for antiglioma treatment. The nanohybrid protein toxin could achieve brain targeting through LF-mediated BBB penetration to reach the tumor site, and preferentially activated by the glioma-associated MMPs, thus triggering CPP-assisting intratumoral infiltration and cell penetration. The rTLM-LF enhanced the antiglioma activity and reduced the systematic toxicity and immunogenicity. Our method provide a feasible strategy for improving the drug-like property of protein toxins. Furthermore, it offers a potential solution for achieving glioma dual-targeting delivery of therapeutic proteins and macromolecular therapy of glioma.

Experimental section

Materials

The original TCS plasmid was kindly provided by Prof. Pang-Chui Shaw (The Chinese University of Hong Kong). *E.coli* strain BL21 (DE3) was preserved by our laboratory. The IMPACT (Intein-mediated purification with affinity chitin-binding tag) system, including the expressing vector pTXB1 and chitin resin, was obtained from New England Biolabs (UK). Lysogeny Broth (LB) medium was purchased from Oxoid (UK). N-hydroxysuccinimide-PEG$_{3500}$-Maleimide (NHS-PEG-MAL) was acquired from Jenkem Technology Co., Ltd (Beijing, China). Protein marker and isopropyl β-D-thiogalactopyranoside (IPTG) were acquired from Thermo Scientific (USA). Bovine lactoferrin was obtained from Titan Technology Co., Ltd (Shanghai, China). Murine glioma cell line GL261 and C6, murine brain capillary endothelium cells (BCEC), human ovarian cancer cell line HeLa and human breast cancer cell line MCF-7 were gained from Cell Bank of Chinese Academy of Sciences. Fetal bovine serums (FBS), RPMI 1640 medium, Dulbecco's modified Eagle's Medium (DMEM) cell culture medium and 0.25% trypsin-EDTA were purchased from Gibco (USA). BCA microplate protein assay kit was obtained from Beyotime Institute of Biotechnology (Haimen, China). 3-(4, 5-Dimethylthiazol-2-yl)-2, 5-diphenyltetrazolium bromide (MTT) and cocktail protease inhibitor were purchased from Sigma-Aldrich Co., Ltd (USA). All antibiotics were acquired from Amresco (USA). L-cysteine was obtained from J&K Scientific Ltd (Shanghai, China). NHS-Cy5 and fluorescein isothiocyanate (FITC) were obtained from Melonepharma Biotechnology Co., Ltd (Dalian, China). All other reagents were of analytical grade from Sinapharm Chemical Reagent Co., Ltd. (Shanghai, China).

Protein expression and purification

The nucleotide sequence encoding LMWP (VSRRRRRRGGRRRR) and MMP-2 substrate peptide (MSP, PLGLAG) were added to the 3′-end of TCS-encoding gene by PCR method to form fusion gene TCS-LMWP-MSP (TLM). TCS- or TLM-encoding gene was then subcloned into the intein-mediated

protein expressing vector pTXB1 at NdeI/XhoI site to construct recombinant plasmid pTCS and pTLM.

Recombinant plasmid pTCS or pTLM was transformed into *E.coli* BL21 (DE3) competent cells. Bacteria were cultured in LB medium containing 100 µg/ml Ampicillin at 250 rpm in a 37°C shaker. When OD_{600nm} approached about 0.6, IPTG was added at a final concentration of 0.3 mM to induce the target protein expression. The expression of recombinant TCS (rTCS) or TCS-LMWP-MSP (rTLM) was induced overnight at 23°C and 150 rpm. Bacteria were harvested by centrifuge at 8,000 rpm for 20 min, and then suspended in the column buffer (20 mM HEPES-sodium, 500 mM NaCl, 1 mM EDTA, pH 8.5), and lysed by using ultrasound. After cell pellet was removed by centrifuge at 12,000 rpm for 30 min, the bacterial lysate was loaded onto a pre-equilibrated chitin gravity column. The column was then flushed with the column buffer to remove non-specific binding proteins, followed by the addition of 6 column volumes of cleavage buffer (50 mM of L-cysteine in column buffer). The column was incubated with cleavage buffer to perform intein-mediated cleavage at 4°C for 16 h to yield the target protein rTCS or rTLM with a C-terminal cysteine. After elution and collection from the chitin column, the product was condensed by ultrafiltration (MWCO 10 k, Millipore, USA), followed by further purification using FPLC system (GE Healthcare, USA) equipped with a desalting column (HiTrap Desalting, GE Healthcare, USA) to remove excess cysteine.

Preparation of rTLM-LF

Lactoferrin (LF) was chemically conjugated with rTLM using a hetero-bifunctional PEG as a cross-linker. Maleimide-activated LF was prepared by mixing LF with 5-molar excess of NHS-PEG-MAL in 20 mM phosphate sodium buffer (PBS, pH 7.2) for 1-h incubation at room temperature. The excess PEG was removed by using a desalting column. The rTLM fusion protein with a C-terminal cysteine was mixed with 5-molar excess of the maleimide-activated LF in PBS to react at 4°C for overnight. Therefore, the LF could be site-specially conjugated to the rTLM C-terminus via the PEG linker.

The rTLM-LF was separated from unreacted rTLM and LF using a cation-exchange column (HiTrap SPFF, GE Healthcare, USA) with a salt gradient elution from 0.05 to 1 M NaCl in 10 mM Tris-HCl (pH 8.0) buffer at a rate of 0.02 M/min and a flow rate of 1 ml/min. The purified rTLM-LF was characterized by SDS-PAGE electrophoresis and atomic force microscopy (AFM). The desalted samples (LF and rTLM-LF) were dropped onto the mica sheets and then dried by incubating at 30°C for 20 min before subjected to AFM analysis (Dimension Icon, Bruker, USA).

Cell culture

BCEC, GL261 and C6 murine cells were cultured in 25 cm² flasks and maintained in DMEM in a humidified 5% CO_2 incubator at 37°C. Human ovarian cancer cell line HeLa and human breast cancer cell line MCF-7 were cultured in RPMI 1640 medium. All cell culture medium contained 10% FBS, 100 IU/ml penicillin and 100 µg/ml streptomycin (Amresco, USA).

Fluorescent labeling of proteins

Proteins were labeled with 20-molar excess of FITC or 3-molar excess of NHS-Cy5 at 4°C for overnight. The excess of the fluorescent dye was removed by subjected to a desalting column (HiTrap Desalting, GE Healthcare, USA) and an FPLC system (GE Healthcare, USA).

Evaluation of rTLM-LF penetration across BBB

BCEC cells were seeded into 12-well plate with a density of 1×10^5 cells per well 24 h before treatment. The cells were treated with the FITC-labeled rTCS or rTLM-LF (2 µM) and incubated at 37°C for 4 h. In parallel, the cells pretreated with 20 µg/ml LDL or 50 µM free LF for 2 h were treated with 2 µM rTLM-LF and incubated under the same condition. After cell medium was discarded, the cells were washed with PBS and heparin-sodium subsequently to remove non-specific cell surface-binding proteins. Cellular uptake of rTCS or rTLM-LF was imaged by fluorescent microscopy (Zeiss, Germany). Moreover, the cells were digested by trypsin, and analyzed using flow cytometry (BD Pharmingen, USA).

BCEC cells were seeded into the upper chambers of Transwell cell culture plate (Corning, USA) at a density of 1×10^5 cells per chamber 96 h before treatment. The integrity of the BCEC cells was tested by measuring the transepithelial electrical resistance (TEER) (>200 Ω•cm²). GL261 cells were seeded into the lower chambers at a density of 5×10^4 cells per chamber 24 h before treatment, thus developing an *in vitro* BBB cell culture model. The BCEC cells in the upper chambers were treated with the FITC-labeled rTCS or rTLM-LF (10 µM) and incubated at 37°C for 4 h. Cells pretreated with LDL or LF as the same method as described above were incubated with rTLM-LF (10 µM) in parallel. Cellular uptake of rTCS and rTLM-LF in GL261 cells were observed and analyzed using fluorescent microscopy (Zeiss, Germany). At the meantime, the cells treated with the same procedures were collected and analyzed using

flow cytometry (BD Pharmingen, USA).

In vitro cytotoxicity study

The *in vitro* anti-cancer activity of rTCS, rTLM-LF, rTLM, and unmodified LF were determined by a standard MTT assay in C6 and GL261 glioma cells, and normal cells such as BCEC and HUVEC cells. The cells were seeded to 96-well plates at a density of 3,000 cells per well 24 h before treatment. The cells were exposed to various concentrations of protein toxins for 48 h. Subsequently, 20 μl of MTT (5 mg/ml) solution was added to each well and incubated for additional 4 h. The medium was carefully removed and 200 μl of DMSO was added to each well to dissolve the formazan crystals. The absorbance was measured using a microplate reader (Thermo Scientific, USA) at $\lambda_{570\ nm}$. The relative cell viability was calculated according to the following equation:

Cell viability (%) = (OD$_{test}$ - OD$_{DMSO}$) / (OD$_{control}$ - OD$_{DMSO}$) × 100%

MMP-2-mediated cleavage assay

MMP-2-mediated cleavage of rTLM-LF was conducted using the GL261-conditioned medium. GL261 cells were seeded into a 60-mm dish with a density of 4×10^6 cells. After cells adhered to the dish, the culture medium was replaced with fresh medium without FBS. After 24-h incubation, the medium was collected and centrifuged at 12,000 rpm for 10 min at 4°C to remove the cell debris. The rTLM-LF was incubated with the prepared GL261-conditioned medium at 37°C for 24 h. MMP-2-mediated cleavage efficiency of rTLM-LF was assessed by SDS-PAGE electrophoresis, and analyzed by gray scale analysis using ImageJ.

Western blotting assay

The GL261 and C6-conditioned mediums were prepared as described above. The GL261, C6, BCEC, bEnd.3 and HUVEC cells were lysed by using RIPA lysate buffer containing cocktail protease inhibitors. Total protein concentration of the cell lysate and medium was determined by BCA protein assay, and adjusted to the same protein concentration. All samples were loaded to 10% SDS-PAGE electrophoresis and electrotransferred to PVDF membranes (Millipore, USA). After blocked by 5% BSA, the membranes were incubated with anti-MMP-2, anti-LRP-1 (Abcam, UK) and anti-β-actin (Sigma-Aldrich, USA) monoclonal antibody at 4°C for overnight, and HRP-labeled secondary antibody (Santa Cruz, USA) at room temperature for 1 h. The membrane was incubated with ECL substrate solution (Peirce, USA) and then subjected to a gel-imaging

system (Biorad, USA).

Cellular uptake assay of rTLM-LF and rTLM

C6 and GL261 cells were seeded into a 12-well plate at a density of 1×10^5 cells per well 24 h before treatment. The cells with or without pretreatment with LF were incubated with FITC-labeled rTLM-LF and rTLM (2 μM) at 37°C for 4 h, and collected by trypsin digestion for flow cytometry analysis of the fluorescent intensity to evaluate the cellular uptake level.

MMP-2-mediated cellular uptake

FITC-labeled rTLM-LF was pretreated with the GL261-conditioned medium at 37°C for 24 h. GL261, C6, HeLa, and MCF-7 cells were seeded into a 12-well plate at a density of 1×10^5 cells per well 24 h before treatment. The cells were incubated with rTLM-LF or pre-cleaved rTLM-LF (2 μM) at 37°C for 4 h, followed by 4% paraformaldehyde fixing and DAPI staining. The cellular uptake efficiency was observed by using fluorescent microscopy and determined using flow cytometry as described above.

Animal experiments

All the animal experimental procedures were approved by the IACUC. All experimental animals housed under specific pathogen-free (SPF) condition were free to access sterilized food pellets and distilled water with a 12-h light/dark cycle.

In vivo imaging

The orthotopic glioma model was established on the male Balb/c nude mice (6-week old) by intracranial injection of approximately 5×10^5 GL261 cells into the right cerebrum. The GL261-bearing mice were intravenously injected with the Cy5-labeled rTCS or rTLM-LF seven days after tumor inoculation. The *in-vivo* brain targeting of rTCS or rTLM-LF was imaged by IVIS imaging system (Caliper Life Science, USA) 24 h post-dose. The mice were humanely sacrificed and the major organs (e.g., heart, liver, spleen, lung and kidney) and brains were collected for imaging to investigate the bio-distribution of rTCS and rTLM-LF.

The cryosection slices of the brain were fixed in 4% paraformaldehyde, and processed immunofluorescence staining by using the rabbit anti-LRP-1 monoclonal antibody (Abcam, UK) and FITC-labeled goat anti-rabbit secondary antibody (Santa Cruz, USA). The tissue slices were imaged using a confocal laser scanning microscope (Olympus, Japan).

In vivo treatment study

Subcutaneous glioma model: the male Balb/c nude mice (6-week old) were subcutaneously

implanted with 1×10^7 GL261 cells, and randomly divided into four groups (five per group). When the tumor size reached about 150 mm³, the animals were given saline, rTCS (100 nmol/kg, q.o.d.), and rTLM-LF (50 nmol/kg or 100 nmol/kg, q.o.d.), respectively, via tail vein injection over a period of 18 days. The male C57BL/6 mice, implanted with GL261 cells with the same method, were randomly divided into three groups (four per group). When the tumor size reached about 150 mm³, the animals were given saline, rTCS (100 nmol/kg, q.o.d.), and rTLM-LF (100 nmol/kg, q.o.d.), respectively, via tail vein injection over a period of 24 days. The anticancer therapeutic efficacy was evaluated by monitoring the tumor size. The tumor size was calculated according to the following formula:

$$V = (W^2 \times L) / 2$$

where L is the longest diameter and W is the shortest diameter.

During the treatment course, the animal body weights were monitored. At the experimental endpoint, the animals were humanely sacrificed and tumors were collected and weighed.

The lymph nodes and spleens of C57BL/6 mice were collected and grinded into single cells. After the red blood cells (RBC) were lysed using RBC lysate buffer, cells were blocked by Fc receptor blocker and stained by PerCP--anti-CD3ε antibody, FITC--anti-CD4 antibody and APC--anti-CD8α antibody (BD Pharmingen, USA). The percentage of CD4+ and CD8+ T cells were analyzed using a flow cytometer (Calibur, BD Pharmingen, USA). The CD8+ T cell infiltration was evaluated by immunohistochemistry staining of the tumor tissues using anti-CD8α antibody (Novus, USA).

Orthotopic glioma model: The therapeutic efficacy of rTLM-LF was further investigated using the GL261 orthotopic glioma model established on the male Balb/c mice (6-week old) as described the subsection above. The GL261-bearing mice randomly divided into three groups were given saline (n = 7), rTCS (n = 10), and rTLM-LF (n = 10) at an intravenous dose of 100 nmol/kg (q.o.d.). The survival rate and animal body weight change were recorded to evaluate the antiglioma therapeutic efficacy. In another parallel experiment, orthotopic GL261-xenografted mice, grouped by the same method, were given saline, rTCS (100 nmol/kg), and rTLM-LF (100 nmol/kg) for consecutive three days. The animals were then humanely sacrificed, and the brains and major organs (liver, spleen, lung and kidney) were collected for H&E staining and pathologic analysis. The blood samples were also collected for detection of plasma AST/ALT and ALP levels to evaluate the hepatotoxicity.

Immunogenicity

Female Balb/c mice (6-week old) were divided into three groups (five per group): rTCS, rTLM-LF, and rTCS-PEG. The animals were immunized at a dose of 10 μg protein per animal subcutaneously once every week for three times. Blood samples of each animal were collected from retro-orbital sinus seven days after the last immunization and serum were separated by centrifuge. The titer of anti-TCS IgG in serum samples was detected by ELISA assay. Briefly, rTCS was diluted by 50 mM bicarbonate buffer (pH 9.6) to 10 μg/ml and was coated to the bottom of a 96-well high-binding ELISA plate (Santa Cruz, USA) with 100 μl per well for 18 h at 4°C. After washing with PBS-T for three times, the plate was blocked by PBS-T containing 1% BSA at 37°C for 1.5 h. Serum samples were diluted by PBS-T containing 0.01% BSA to 1:1,000–1,000,000. The diluted serum sample (100 μl/well) was dispensed and incubated at 37°C for 1 h. After washing three times, each well was incubated with 100 μl of the HRP-labeled goat anti-mouse secondary antibody (Santa Cruz, USA) diluted by 1,000 folds for 1 h. After secondary antibody was washed by PBS-T for three times, 200 μl of TMB substrate solution was added to each well and incubated for 15 min at 37°C. The chromogenic reaction was terminated by adding 50 μl of 20% H_2SO_4 to each well. The absorbance was measured using a microplate reader at λ = 450 nm.

Statistical analyses

The results were shown as mean ± SD (n>3). Statistical analysis was conducted using ordinary one-way ANOVA test by GraphPad Prism. Survival analysis was conducted using Log-range (Mantel-Cox) test by GraphPad Prism. *p<0.05; **p<0.01; ***p<0.001.

Acknowledgment

Supplementary Material

Supplementary figures.
http://www.thno.org/v07p3489s1.pdf

Competing Interests

The authors have declared that no competing interest exists.

References

1. Brown RC, Morris AP, O'Neil RG. Tight junction protein expression and barrier properties of immortalized mouse brain microvessel endothelial cells. Brain Res. 2007; 1130: 17-30.
2. Lo EH, Singhal AB, Torchilin VP, Abbott NJ. Drug delivery to damaged brain. Brain Res Brain Res Rev. 2001; 38: 140-8.
3. Sha O, Niu J, Ng TB, Cho EY, Fu X, Jiang W. Anti-tumor action of trichosanthin, a type 1 ribosome-inactivating protein, employed in traditional Chinese medicine: a mini review. Cancer Chemother Pharmacol. 2013; 71: 1387-93.
4. Fang EF, Zhang CZY, Zhang L, Wong JH, Chan YS, Pan WL, et al. Trichosanthin Inhibits Breast Cancer Cell Proliferation in Both Cell Lines and Nude Mice by Promotion of Apoptosis. PLOS ONE. 2012; 7: e41592.
5. Pardridge WM. Biopharmaceutical drug targeting to the brain. J Drug Target. 2010; 18: 157-67.
6. Wang P, Xu J, Zhang C. CREB, a possible upstream regulator of Bcl-2 in trichosanthin-induced HeLa cell apoptosis. Mol Biol Rep. 2010; 37: 1891-6.
7. Liu F, Wang B, Wang Z, Yu S. Trichosanthin down-regulates Notch signaling and inhibits proliferation of the nasopharyngeal carcinoma cell line CNE2 *in vitro*. Fitoterapia. 2012; 83: 838-42.
8. Li M, Li X, Li JC. Possible mechanisms of trichosanthin-induced apoptosis of tumor cells. Anatomical record. 2010; 293: 986-92.
9. An Q, Lei Y, Jia N, Zhang X, Bai Y, Yi J, et al. Effect of site-directed PEGylation of trichosanthin on its biological activity, immunogenicity, and pharmacokinetics. Biomolecular engineering. 2007; 24: 643-9.
10. Liu Z, Jiang M, Kang T, Miao D, Gu G, Song Q, et al. Lactoferrin-modified PEG-co-PCL nanoparticles for enhanced brain delivery of NAP peptide following intranasal administration. Biomaterials. 2013; 34: 3870-81.
11. Mitchell SF, Lorsch JR. Protein Affinity Purification using Intein/Chitin Binding Protein Tags. Methods Enzymol. 2015; 559: 111-25.
12. Yu HH, Nakase I, Pujals S, Hirose H, Tanaka G, Katayama S, et al. Expressed protein ligation for the preparation of fusion proteins with cell penetrating peptides for endotoxin removal and intracellular delivery. Biochim Biophys Acta. 2010; 1798: 2249-57.
13. Ye J, Shin MC, Liang Q, He H, Yang VC. 15 years of ATTEMPTS: a macromolecular drug delivery system based on the CPP-mediated intracellular drug delivery and antibody targeting. J Control Release. 2015; 205: 58-69.
14. Wang H, Zhao Y, Wang H, Gong J, He H, Shin MC, et al. Low-molecular-weight protamine-modified PLGA nanoparticles for overcoming drug-resistant breast cancer. J Control Release. 2014; 192C: 47-56.
15. Lin T, Zhao P, Jiang Y, Tang Y, Jin H, Pan Z, et al. Blood-Brain-Barrier-Penetrating Albumin Nanoparticles for Biomimetic Drug Delivery via Albumin-Binding Protein Pathways for Antiglioma Therapy. ACS Nano. 2016; 10: 9999-10012.
16. Cai Y, Xiong S, Zheng Y, Luo F, Jiang P, Chu Y. Trichosanthin enhances anti-tumor immune response in a murine Lewis lung cancer model by boosting the interaction between TSLC1 and CRTAM. Cellular & molecular immunology. 2011; 8: 359-67.
17. He XH, Shaw PC, Tam SC. Reducing the immunogenicity and improving the *in vivo* activity of trichosanthin by site-directed pegylation. Life Sci. 1999; 65: 355-68.
18. Reyes AG, Anne J, Mejia A. Ribosome-inactivating proteins with an emphasis on bacterial RIPs and their potential medical applications. Future microbiology. 2012; 7: 705-17.
19. Qiu N, Liu X, Zhong Y, Zhou Z, Piao Y, Miao L, et al. Esterase-Activated Charge-Reversal Polymer for Fibroblast-Exempt Cancer Gene Therapy. Adv Mater. 2016; 28: 10613-22.
20. Liu X, Xiang J, Zhu D, Jiang L, Zhou Z, Tang J, et al. Fusogenic Reactive Oxygen Species Triggered Charge-Reversal Vector for Effective Gene Delivery. Adv Mater. 2016; 28: 1743-52.
21. Su Z, Xing L, Chen Y, Xu Y, Yang F, Zhang C, et al. Lactoferrin-modified poly(ethylene glycol)-grafted BSA nanoparticles as a dual-targeting carrier for treating brain gliomas. Mol Pharm. 2014; 11: 1823-34.
22. Qiao R, Jia Q, Huwel S, Xia R, Liu T, Gao F, et al. Receptor-mediated delivery of magnetic nanoparticles across the blood-brain barrier. ACS Nano. 2012; 6: 3304-10.
23. Chen Y, Zhang M, Jin H, Tang Y, Wang H, Xu Q, et al. Intein-mediated site-specific synthesis of tumor-targeting protein delivery system: Turning PEG dilemma into prodrug-like feature. Biomaterials. 2017; 116: 57-68.
24. Chen Y, Zhang M, Jin H, Tang Y, Wu A, Xu Q, Huang Y. Prodrug-Like, PEGylated Protein Toxin Trichosanthin for Reversal of Chemoresistance. Mol Pharm. 2017, 14: 1429-1438